Signal processing in microwave optics by
means of multiple modulated scatterers -
Application to a microwave
image scanning system

J.-G. Wegrowe

IPP 2/77   April 1969

INSTITUT FÜR PLASMAPHYSIK

GARCHING BEI MÜNCHEN

INSTITUT FÜR PLASMAPHYSIK

GARCHING BEI MÜNCHEN

Signal processing in microwave optics by
means of multiple modulated scatterers -
Application to a microwave
image scanning system

J.-G. Wegrowe

IPP 2/77   April 1969

Abstract

It is shown that using an array of modulated scatterers allows
to perform a variety of operations on an optical signal, in a
way similar to holography. As an application a microwave image
scanning system is described in detail. It permits the
exploration of a microwave field with a single fixed receiver
without loss of spatial resolution with regard to the
corresponding purely optical device, and with a good time
resolution. Preliminary experimental results obtained with
such a device are given.

Introduction

Microwave field measurements by means of a modulated scatterer may be generalized using a complete array of modulated scatterers (or a continuous scattering surface). We first examine different techniques for the measurement of microwave fields in sections 1 (point to point measurements) and 2 (measurements of two dimensional field distributions). Section 3 describes the principle and potentialities of the M.M.S. technique (multiple modulated scatterers). The fourth section is devoted to the analysis of a Microwave Image Scanning System (MISS) applying the above mentioned technique. (The foreseen application is a time and space resolved plasma diagnostic). In section 5 preliminary experimental results are given.
We found it convenient to develop in a separate appendix a theory of coherent imaging adapted to the MMS technique.

1. Point-by-point measurements of microwave fields

One may separate the point-by-point field measurements into two groups: the direct measurements and the measurements of the field scattered by a small object.

1.1. In the first group, a receiving aerial is placed at the point where the field is to be measured. This procedure is well adapted to the case of far field measurements whereas for near zone fields special attention must be paid to possible interactions of the receiver with the sources of the field and/or reflecting objects [1]. On the other hand, one must take into account the directivity of the aerial, what is readily done in the measurement in the far zone thanks to the existence of a privileged direction (field point to the source) in which the receiver is directed throughout the measurement. For near zone measurements, a more complicated interaction takes place between the field and the receiver.

Moreover, it is not always possible to put a receiver at the

place where one wishes to measure the field: this is the case in plasma diagnostics where a plasma slab (or column) is illuminated by a wave whose changes after traveling through the plasma must be measured. It is then convenient to use an optical imaging system and to analyze the field distribution in the conjugate plane of the initial distribution [2] (object distribution). Figure 1 shows applications of the "direct" and optical imaging measuring systems.

1.2. The second group of methods consists in the measurement of the field scattered by a small object placed in the field (e.g. dipole or loop). The scattered field at a remote point is then proportional to some component of the unperturbed field(tangential component of the electric field in the case of a small dipole).In an ingenious application [3] one measures the scattered field at the source antenna itself. Making use of the reciprocity theorem one shows that the scattered signal is proportional to the square of the field to be measured independently of the distance source scatterer or of isotropic inhomogeneous interposed media (fig.1). Moreover, the phase comparison does not require then a displacement of a reference guide as in the preceding systems.

To allow a separation between the useful signal and other fields scattered by neighbouring objects, spinning objects or small modulated diodes have been used [4, 5] to build dipoles or loops. One may consider the modulated diodes as antennas with variable load impedance; they provide therefore a modulation of the scattered signal.

2. Measurement of surface field distributions and optical data processing

The above mentioned methods yield amplitude and phase of the field at a given point. A mechanical system may be used to perform an exploration of a whole surface. A good accuracy has been reached this way, but at the expense of a very lengthy procedure [6].

Attempts to get direct visible displays of a field distribution have succeeded recently.Some interesting photographic techniques[7,8]

do not, however, seem until now to be applicable for high speed measurements.

Two other promising techniques have been reported. One of them makes use of the newly available "liquid crystals" whose molecular ordering depends strongly on the temperature [9, 10]. Microwave energy absorbed by a thin film of such a substance gives rise to localized color changes of the visible light reflected from the film (Bragg interferences).

In another approach [11] the microwave image is formed on the surface of a semi-conductor plate whose resistivity (hence transparency to microwave) is locally modulated by light - a single receiver is then used to collect the energy which travelled through the high transparency zones of the plate.

To get both time and space resolution, one may also think to multiply the number of receivers in the image plane. But this would result in an increasingly complicated, expensive and field-disturbing operation as one increases the number of measuring points.

On the other hand, the use of multiple modulated scatterers and a single receiver does not seem to be subject to such strong limitations. Furthermore, by choosing different locations of an array of scatterers in an optical system as well as different types of modulation of the elements, new interesting possibilities are offered which allow to perform besides image exploration a number of other optical image processings.

3. Principle of operation of the systems using multiple modulated scatterers

The leading idea for all the proposed systems is to convert a spatial information into a temporal one by means of an adequately chosen modulation.

Consider a "punctual" modulated microwave scatterer (say a diode of small dimensions compared to the wave length, modulated through thin leads by an externally applied low frequency voltage).

The information attached to that point of space where the scatterer has been located (in the example: amplitude and phase of

one component of the electric field) will be reradiated in the
whole space under modulated form. If several scatterers are
working simultaneously in different points one will be able, by
measuring the total field at a remote point, to recognize
that part contributed by a given field point thanks to its
specific modulation (taking into account the microwave phase and
amplitude corrections due to the different paths between the
given scatterer and the measuring point). Moreover, instead of
separating the elementary informations coming on the receiver,
it is possible to combine them to get the result of different
operations on space (such as integration, Fourier transform,
filtering, translation of an image etc....). This result depends
on one hand on the type of the chosen modulation (i.e. the
chosen correspondence between the space reference system and
time - or frequency reference system) and on the other hand on
the features of the optical device placed between the scatterer
and the receiver.

To illustrate some of these possibilities, let us consider
the following simplified model. The array of modulated scatterers
will be regarded as a continuous plane in which each point is
able to perform a phase modulation of the field. The modulation
of each point is controlled by an external channel (e.g.:L.F.
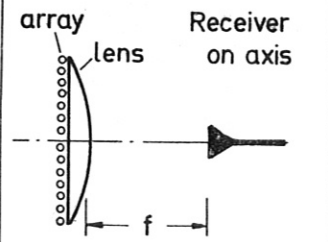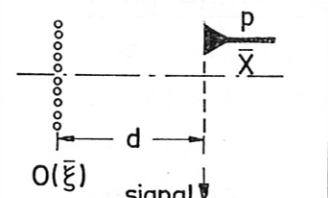voltage, electron beam, light beam, acoustic waves, etc..,
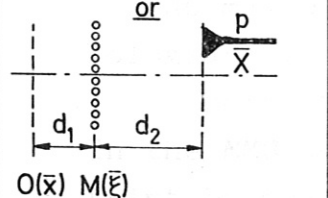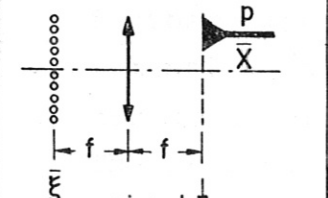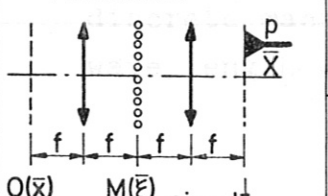examples [11, 12, 13]).

As a further simplification here consider first a one
dimensional case. The array is placed in the plane of a given
distribution (the "object" plane). Let us consider for example
a set-up in which a lens is placed closely to the array and
the receiver at the focus of the lens.

If each point of the array is now modulated by a "sine"
wave $e^{2\pi i F t}$ everywhere with the same phase, the complex signal
on the receiver is then

$$S(t) = \int O(x) \, e^{2\pi i F t} \, dx$$

so that amplitude and phase of the modulated wave are those of
the integral of the field $O(x)$ in the plane of the array.

Table I

OPTICAL SET UP FOR:	M.M.S. FUNKTION: $M(\xi)$	MEASURED AMPLITUDE (MODULATED PART OF SIGNAL)	RESULT OF THE OPERATION
1) INTEGRATION array　　Receiver 　lens　　on axis $\longleftarrow f \longrightarrow$ object plane │ signal $O(\bar{x}) \quad \int O(\bar{\xi}) M(\bar{\xi},t)d\bar{\xi}$	11) $\delta[\bar{\xi}-\bar{\xi}_0(t)]$	$O[\bar{\xi}_0(t)]$	Space exploration displayed over time.
	12) $e^{i\left[\frac{\omega t\,\xi}{\xi_0},\frac{\Omega t\,\eta}{\eta_0}\right]}$	$\tilde{O}\left(\frac{\omega t}{2\pi\xi_0},\frac{\Omega t}{2\pi\eta_0}\right)$	Time display of the f.T. of a two-dimensionnal distribution.
	13) $f(\bar{\xi}-\bar{a}t)$	$O(\bar{a}t)*f(\bar{a}t)$	Time display of the convolution product of two 2D. distributions.
2) FRESNEL-TRANSF. $\longleftarrow d \longrightarrow$ $O(\bar{\xi})$ signal $G_d(\bar{X}) \; F_{\frac{\bar{X}}{\lambda d}}[O(\bar{\xi})M(\bar{\xi},t)G_d(\bar{\xi})]$ **or** $d_1 \quad d_2$ $O(\bar{x}) \; M(\bar{\xi})$	21) $\delta[\bar{\xi}-\bar{\xi}_0(t)]$	$G_d^*[\bar{X}-\bar{\xi}_0(t)]O[\bar{\xi}_0(t)]$ with $G_d(\bar{\xi})=e^{-\pi i \bar{\xi}^2/\lambda f}$	Time display of a 2D space distribution (times a Fresnel phase factor).
	22) $e^{i\left[\pi\frac{\xi^2}{\lambda f}+\pi\frac{\eta^2}{\lambda f}\right]}$ with $\frac{1}{d_1}+\frac{1}{d_2}=\frac{1}{f}$	$G_{d_2}(\bar{X})\,G_{d_1}\left(\bar{X}\frac{d_1}{d_2}\right)O\left(-\bar{X}\frac{d_1}{d_2}\right)$	Lensless optics – (modulating by a real function of space introduces an out - of - focus image).
	23) $e^{i\left[\pi\frac{\bar{\xi}^2}{\lambda f}+\frac{\bar{\omega}t\bar{\xi}}{\xi_0}\right]}$ with $\frac{1}{d_1}+\frac{1}{d_2}=\frac{1}{f}$	$G_{d_2}(\bar{X})\,G_{d_1}\left(-\bar{X}\frac{d_1}{d_2}+\frac{\bar{\omega}t}{2\pi}\frac{\lambda d_2}{\xi_0}\right)\cdot$ $\cdot\,O\left(-\bar{X}\frac{d_1}{d_2}+\frac{\bar{\omega}t}{2\pi}\frac{\lambda d_2}{\xi_0}\right)$	Lensless optics allowing a time display of a 2D space distribution.
3) FOURIER-TRANSFORM $\longmapsto f \longrightarrow\longmapsto f \longrightarrow$ $\bar{\xi}$ signal $\widetilde{OM}\left(\frac{\bar{X}}{\lambda f}\right)$	31) $\delta[\bar{\xi}-\bar{\xi}_0(t)]$	$O(\bar{\xi}_0)e^{2\pi i\bar{X}\bar{\xi}_0(t)/\lambda f}$	Time display of a 2D space distribution (times a Fourier phase factor).
	32) $e^{-i\bar{\omega}t\bar{\xi}}$	$\tilde{O}\left(\frac{\bar{X}}{\lambda f}\,\frac{\bar{\omega}t}{2\pi}\right)$	Time display of the F.T. of a 2D distribution.
	33) $f(\bar{k}\bar{\xi}-\omega t)$ (a travelling wave)	$\delta\left(\frac{N}{\lambda f}\right)\bar{e}^{2\pi i\frac{M\omega t}{k\lambda f}}\tilde{f}\left(\frac{M}{k\lambda f}\right)$ N length in a direction perpendicular to $\vec{k}$ M length in a dir. parallel to $\vec{k}$	Display along the direction of $\bar{k}$ of the function $\tilde{f}$ with a frequency proportional to the velocity of the wave packet.
4) FOURIER-PLANE FILTERING $\|f\|f\|f\|f\|$ $O(\bar{x}) \quad M(\bar{\xi})$ signal $[\tilde{M}*O]\left(\frac{\bar{X}}{\lambda f}\right)$	41) $\delta[\bar{\xi}-\bar{\xi}_0(t)]$	$e^{2\pi i\frac{\bar{X}\bar{\xi}_0}{\lambda f}}$	
	42) $e^{i\frac{\bar{\xi}\bar{\omega}t}{\xi_0}}$	$O\left(\bar{X}-\frac{\bar{\omega}t}{2\pi}\frac{\lambda f}{\xi_0}\right)$	Time display of a 2D distribution.

In the same set-up, if each point is now modulated by a sine wave whose frequency is proportional to the abscissa:

$$e^{2\pi i \, F \times t / x_0}$$

one gets

$$S(t) = \int O(\bar{x}) \, e^{2\pi i \, F \frac{x}{x_0} t} \, dx = \widetilde{O}\left(\frac{Ft}{x_0}\right)$$

Now, amplitude and phase of the received microwave signal are those of the Fourier-transform $\widetilde{O}$ of the initial field distribution: the <u>time</u> dependence of the microwave signal reflects the <u>spatial frequency spectrum</u> of the object. In table I some other possibilities are schematically shown, examplifying the potential possibilities of the Multiple Modulated Scatterers technique. Among these applications let us quote: image scanning; lensless imaging (with electrical variations of the focus); spatial dispersion of a signal...

As may be seen, the MMS technique bears resemblance to holography. Their common point is the mixing occuring at each point of a signal distribution with a reference distribution. In the MMS technique, the reference is brought on each space point by means of an independent channel (electrical or of any other nature) whereas in holography the reference is given by a second optical signal. This may allow to use in MMS a wide variety of signal structures (e.g. example 33 in table I). A further important difference is the availability in MMS of the dimension "time" which is frozen in holography because of the necessity of processing the film before reconstructing the image. The presence of twin images in holography (due to the non linear effect of the film sensitivity) has its corresponding disagreement in MMS if no true phase modulation may be obtained from the scatterers.

It should also be noticed here that the MMS technique may be easily applied in the microwave range where even discrete scatterers may be used without loss of resolution. Conversely discrete macroscopic scatterers could be used even with shorter wave length where resolution is not demanded.

In the next section the application to microwave image
scanning (cases 1.1 .and 4.2 .of table I) will be discussed in
detail.

4. The microwave image scanning system (MISS)

The basic element of this system is an array of scatterers
disposed at the intersections of $2N_x+1$ equally spaced columns and
$2N_y+1$ equally spaced lines

We use the property of a small isolated scatterer to give
rise to a scattered field distribution whose complex amplitude
is proportional to that of the (unperturbed) field at the place
where the scatterer is located.

Moreover, we make the following assumptions:

i)   The scatterers of the array are identical:

ii)   The perturbation due to the rest of the
      array at the place of one scatterer is small
      compared with the incident field:

iii) Multiple scattering processes may be neglected
      (because of the weakness of the modulated part
      of the scattered field compared with the
      incident field):

iiii) The modulated part of the scattered field due
      to one scatterer will be considered as zero
      everywhere except on the scatterer itself
      (this insures   the fulfillment of (iii)).
      This assumption simplifies the calculations
      but is not essential.

4.1. Point by point exploration of a field with the array (cases 1.1. and 3.1. of table I)

In order to receive comparable informations from each scatterer,
the optical paths from the different scatterers to the receiving
aerial should be the same. This condition will be fulfilled by
means of a lens placed either closely behind the array and through

which a plane wave impinging on the array side parallel to
the axis if focused on the receiver R (equation (27) of
the appendix shows then the direct proportionality between
the scattered signal and the received signal) or placed as
shown in 31, table I (eq.95 of appendix). The signal on the
receiver is detected by a crystal and displayed as intensity
modulation of the light spot on the screen of an oscilloscope.
The coordinates of the spot on the screen are made proportional
to those of the successively working scatterer of the array.
If a strong constant signal is added to the small modulated
one, the detector detects linearly the modulated field and
gives a signal proportional to its amplitude times the cosinus
of the phase angle between the modulated field and the strong
constant one. (A not modulated signal is already present in
the cases of 1.1. and 3.1.,table I , because part of the
unmodulated field also comes on the receiver).

There are disadvantageous features of this kind of
exploration. Firstly, it is difficult to match perfectly the
condition i) above (identical scatterers) which results in a
distorted display (see fig. 7). Secondly, the measurment is
not continuous on the image plane so that information may be
rapidly lost for images of detailed objects. We discuss
therefore the other configuration (case 4.2. in table I) which
uses all scatterers simultaneously. Small differences in
efficiency between them are able to cancel out in the result;
furthermore, a continuous display of the image plane is obtained
which allows a better use of the available resolution(corresponding
to the array-receiver aperture ratio).

4.2. Translation of an image through phase multiplication in
the space of the Fourier-transform

Simplifying the results derived in the appendix, we may describe
the principle of operation as follows:

The array of scattering elements is placed in the plane (η_2)
of fig. 2. The field distribution in this plane is equal to the

Fourier transform of the distribution in the focal plane π_1 (eq.(25)). Supposing now the array being able to perform a true phase multiplication of the type

$$e^{2\pi i\,(\alpha x/a\,+\,\beta y/b)}$$

continuously over the whole surface of the aperture in (π_2), it becomes then clear that the distribution in the conjugate plane (π_3) - itself due to a second Fourier transformation of the illumination on (π_2) - will have suffered a simple translation (a multiplication by a linear phase factor in the Fourier space being equivalent to a translation of the function in the space) (see fig. 3). More physically expressed: the phase term above is the one which would describe the action of a small dielectric prism inserted in the back focal plane (π_2).

If the scatterers perform an amplitude modulation $\cos(2\pi\frac{\alpha x}{a} + 2\pi\frac{\beta y}{b})$, then we get in the image plane the sum of two images, each of them being translated of the same amount in opposite directions. By a judicious choice of dimensioning parameters it will be possible, as shown below, to separate these images.

Now, if our scatterers do not work on the whole surface, but only at the nodes of the array: we must multiply again our distribution in (π_2) by a sampling factor (a Dirac comb). Its Fourier transform is also a Dirac comb which must be convolved with the preceding distribution in (π_3) (a product in a space being equivalent to a convolution in the Fourier-transform space). The result is that we get now a multiplicity of contiguous images(this arises because of the array which we superposed in the object plane) - the whole multiplicity being translated as was the image in the case of a spatially continuous modulating factor - see eq.(38).

At this point, we must pay attention to the special nature of the scatterers we used, namely: diodes. There does not seem to be a means to get from diodes a complex phase multiplicating factor of the type

$$e^{2\pi i\,(\frac{\alpha x}{a}\,+\,\frac{\beta y}{b})}$$

or even of the type

$$\cos 2\pi \left(\frac{\alpha x}{a} + \frac{\beta y}{b} \right)$$

suppose for instance that a diode is connected between two wires, respectively at potentials

$$V_1 = \upsilon_1 \cos (\omega t + \varphi)$$

$$V_2 = \upsilon_2 \cos (\Omega t + \psi)$$

the diode would react to their difference and the nonlinearity of the diode, leading only for $V_1 - V_2 > 0$ would then give a very intricated modulating function. Instead, we choose the potentials V_1 and V_2 to be equal and high enough to bring the diode separately to its current saturation in the leading direction. The simultaneous application of the two potentials then leads to a current as shown in fig. 4. Thus the modulating function of each scatterer may then be written

$$S \left[\cos(\Omega t + \delta \Omega t \frac{x}{a}) \right] \cdot S \left[\cos (\omega t + \delta \omega t \frac{y}{b}) \right]$$

where

$$S \left[f(t) \right] \begin{array}{l} = 1 \text{ for} \\ = 0 \text{ for} \end{array} \qquad \begin{array}{l} f(t) > 0 \\ f(t) \leqslant 0 \end{array}$$

For a given value of t this corresponds to a zoned modulation.

To provide the necessary phase distribution over the array, the diodes are fed as shown in fig. 4. Thanks to the small frequency difference from one row to the next the phase difference of the modulating signals between the two rows increases with time starting at zero at time zero where a trigger impulse is fed into the oscillators. Practically, one may consider this modulating factor as a superposition of signals at the fundamental frequencies Ω and ω and at higher harmonics $k\Omega, \ell\omega$ (with k, l positive and negative integers). For each couple $(k\Omega, \ell\omega)$ of frequency components one gets a traveling multiplicity of images as before. The traveling velocity is however proportional to the

order of the considered harmonics (see eq.(42) and the discussion of § A.10 of the appendix). One of these subimages with carrier frequencies $k\Omega$, $l\omega$ has a relative complex amplitude $e^{i(k\Omega + l\omega)t}$. $\sin k\pi/2$. $\sin l\pi/2 / kl\pi^2$ and is translated in the image plane (x, y) by an amount:

$$\Delta x = \left(n + \frac{k\delta\Omega.t}{2\pi}\right) \frac{\lambda f}{a}$$

$$\Delta y = \left(m + \frac{l\delta\omega t}{2\pi}\right) \frac{\lambda f}{b}$$

(m, n) indexes the order of the image given by the array, a and b are the distances between two columns and two lines respectively.

A filtering is then necessary at the output of the receiver which is always possible if the detection is linear (for instance a quadratic detector will perform this linear detection if one adds a strong constant signal to the small modulated one). The filter should be centered on the frequency $\Omega + \omega$ with a sufficient bandwidth to let through the details of the images during the translation (bandwidth BW greater than $2(N_x\delta\Omega + N_y\delta\omega)$ and smaller than $2(\Omega + \omega)$). But this filtering is not enough to get a single image of the object: indeed, the term with $k = l = -1$ gives the same absolute frequency but an image which travels in the opposite direction (this being due to the use of an amplitude modulation rather than to a pure phase modulation. The presence of this "twin-image" has the same origin as in holography as noted before). To get rid of it the simplest procedure is to push the receiver away from the optic axis ("biasing") as shown in fig. 5 and concurrently limiting the field of view to the diameter D_{max} (see figure 5).

Finally, a sufficient attenuation of "cross modulation" products (terms with $|k\Omega \pm l\omega| = \Omega + \omega$) is required.

A display is then obtained by monitoring the intensity of the light spot on the screen of the CRT by the filtered output (phase information is retained by performing a phase detection on the frequency $\Omega + \omega$) whereas the coordinates of the spot are sclaved to $\delta\Omega t$ and $\delta\omega t$.

4.3. Design parameters

The zeroth order image with fundamental carrier frequencies
k = 1, l = 1, was shown to travel in the image plane at a rate:

$$\begin{cases} x(t) = \dfrac{\delta\Omega\, t}{2\pi}\, \dfrac{\lambda f_2}{a} \\[2mm] y(t) = \dfrac{\delta\omega\, t}{2\pi}\, \dfrac{\lambda f_2}{b} \end{cases}$$

Higher order images (if any, i.e. if a or $b > \lambda$) are distant of

$$\Delta x = \frac{\lambda f_2}{a} \qquad , \qquad \Delta y = \frac{\lambda f_2}{b}$$

During the complete exploration of an image, the overlapping
with images of different orders, and with images having k = l = -1,
must be avoided. An adequate location of the receiver would then
be at the point $X_o = \Delta x/4$, $Y_o = \Delta y/4$ (see fig. 5). If the
width of the image is limited to $\Delta x/2, \Delta y/2$, then a complete
exploration in X of the image n = 0, k = 1 occurs in a time
$t = \pi/\delta\Omega$ before the images n = 1, k = -1, and n = -1, k = -1 come
to overlap on the detector with the useful image (this off-axis
tilting of the receiver will be referred to as "spatial biasing").

The available dimensions of the object are then

$$D_x = \lambda f_1/2a \quad , \quad \lambda f_2/2b$$

The protection against the images having as carrier higher
harmonics of the modulating frequencies may be realized through
the common action of the filter and of the spatial biasing. The
filter let through only those terms for which $|k\Omega \pm \ell\omega| = \Omega + \omega$
with a bandwidth restricted to $2(N_x \delta\Omega + N_y \delta\omega)$. The amplitude
of such a term is firstly reduced (according to (41)) by a factor
kl with regard to the useful term. Secondly, the information
content of the sub-image (k,l) is reduced by the filter which
should now have a $BW = 2(k N_x \delta\Omega + l N_y \delta\omega)$ in order to accept
all details of the rapidly travelling sub-image. Thirdly, the
spatial biasing eliminates a great number of these sub-images
(such as for instance n = -2, k = 1, m and l arbitrary) which
during their translation never overlap with the receiver. As
an example, choosing $3\omega = 5\Omega$, the firstly detected perturbating

term is $k = 11$, $l = 5$ having a relative amplitude $\frac{1}{55}$.

Field and resolution:

The biasing implies a restriction on the object field D_x:

$$D_x \leq \lambda f_1 / 2a$$

(which is more severe as the paraxial condition: $D_x < pf_1$ - with, say, $1 < p < 2$ - if we assume $\lambda < 2a$)

To use fully the available field, we choose:

$$D_x = \lambda f_1 / 2a$$

(This is a strong restriction for short wave length for which the distance a between two scatterers would be much greater than λ)

The number of resolved points on the available field: R_x is then (with r the radius of the diffraction pattern: eq.36b)

$$R_x = \frac{D_x}{r} = \frac{\lambda f_1}{2a} \cdot \frac{(2N_x + 1)a}{\lambda f_1} = \frac{2N_x + 1}{2}$$

Hence, the number of resolved points equals half the number of diodes.

The number of theoretically resolved points for the equivalent purely optical device: R_o is

$$R_o = \frac{D_o}{r} = \frac{pf_1}{\lambda f_1} A = \frac{pA}{\lambda} = \frac{2N_x \, pa}{\lambda}$$

(where we replaced the lens aperture by the array aperture $2Na$) yielding

$$\frac{R_o}{R_x} = 2pa/\lambda$$

which indicates the possiblity in the microwave range to avoid any loss of relative resolution of the MISS with regard to a conventional purely optical system.

5. Experimental results

5.1. Point by point exploration

An array of 5 x 6 diodes with glass envelope was used to measure
and display different field distributions. The spacing between
two diodes was 1 cm, vertically and 2 cm horizontally, the
wave length 8,6 mm. The figure 6 shows an exploration of the field
in the focal plane of a dielectric lens illuminated by an open
wave guide as source. Exploration of the field with an open wave
guide and with some diodes of the array is shown. A typical
display of this focal pattern produced by the array on the screen
of an oscilloscope is shown in figure 7a. The spot on the screen
has been broadened. Here, the array has been displaced 1 cm
horizontally between each picture to show the approximate constancy
of the displayed pattern (irregularities in the diode efficiency
are visible). The next figure 7b shows a pattern produced by an
extended source (horn corrected by a lens).

5.2. Continuous exploration by a MISS with array in the Fourier transform plane

A single dimensional exploration of different images was
accomplished by using an array of 5 x 5 diodes 1 cm apart in each
direction (wave length used: 8,6 mm). The experimental set-up
corresponded to this of figure 2 with $f_1 = f_2 = 10$ cm. The
expected number of resolved points on the object is 2.5 and the
limited field in the object plane 4.3 cm. No modulation was
applied along the y direction whereas the carrier frequency $\Omega/2\pi$
was chosen equal to 10 kHz. The feeding frequencies differed about
2 % between two neighbouring diodes so that a total bandwidth
of 10 % was required for the modulating signal. Figure 8 shows
the block diagramm of the modulating and displaying systems.

The overall sensibility of the system was just sufficient to
allow a partly reproducible display as shown in the next figure
(fig. 9). However, the displays correspond fairly well to the
actual images if one takes into account the effective resolving power
and field of this small array.

MISS appendix

A1) Field at a remote point from an aperture

Using the concept of the angular spectrum of plane waves[14]
we represent the field on Π_1, (fig. 2) by its Fourier transform
(F.T.):

$$\widetilde{E}(u,v) = \iint\limits_{-\infty}^{+\infty} E_{\Pi_1}(x,y)\, e^{2\pi i(ux+vy)}\, dx\, dy \qquad (1)$$

E_{Π_1} being the amplitude of the aperture field, supposed to be
polarized along the x-axis.
We introduce here the notations:

$$\widetilde{E}(u,v) \equiv \widetilde{E}(\bar{u}) = \mathcal{F}_{u,v}\left[E_{\Pi_1}(x,y)\right] = \mathcal{F}_{\bar{u}}\left[E_{\Pi_1}(\bar{x})\right]$$

and similarly for the inverse F.T.:

$$E_{\Pi_1}(\bar{x}) = \overline{\mathcal{F}}_{\bar{x}}\left[\widetilde{E}(\bar{u})\right]$$

To each $\bar{u}$ may be associated a plane wave travelling in
vacuum in the direction $\vec{k}_o(\lambda u, \lambda v, \lambda w)$ with the velocity
of light:

$$\lambda^2(u^2 + v^2 + w^2) = 1$$

Hence, summing up these waves once again for $z \neq 0$ after having
multiplied each of them by the appropriated phase and
inclination factors one gets the field in a plane at the
distance z from the aperture plane Π_1:

$$\vec{E}_z(x,y) = \iint\limits_{-\infty}^{+\infty} \frac{w\hat{x} - u\hat{z}}{w}\, \widetilde{E}(u,v)\, e^{-2\pi i(ux+vy+wz)}\, du\, dv \qquad (2)$$

($\hat{x}$ and $\hat{z}$: unit vectors along x and $\mathfrak{z}$ axis respectively).
The $\hat{x}$ component reads:

$$E_{\mathfrak{z}}(\bar{x}) = \overline{\mathcal{F}} \left[\widetilde{E}(\bar{u}) \cdot \Gamma_{\mathfrak{z}}(\bar{u}) \right] \tag{3}$$

where the subscript denotes only the distance along $\mathfrak{z}$, and

$$\Gamma_{\mathfrak{z}}(\bar{u}) = e^{-2\pi i w \mathfrak{z}} = e^{-2\pi i \frac{\mathfrak{z}}{\lambda} \left[1 - \lambda^2 (u^2 + v^2) \right]^{1/2}} \tag{4}$$

Hence, one may represent the remote field as a convolution of
the aperture field E_{ni} , by a function $\gamma_{\mathfrak{z}}(\bar{x})$ as may be seen
by transforming in (3) the F.T. into the convolution product
of the F.T. of the two terms:

$$E_{\mathfrak{z}}(\bar{x}) = E(\bar{x}) * \gamma_{\mathfrak{z}}(\bar{x}) \tag{5}$$

with $\qquad \gamma_{\mathfrak{z}}(\bar{x}) = \overline{\mathcal{F}} \left[\Gamma_{\mathfrak{z}}(\bar{u}) \right] \tag{6}$

A2) Fresnel Transform

If one assumes that the angular spectrum $\widetilde{E}(\bar{u})$ does not
extend too far from the $\hat{z}$ axis, (we shall use this paraxial
approximation throughout this appendix) one may develop $\Gamma_{\mathfrak{z}}$:

$$\Gamma_{\mathfrak{z}}(\bar{u}) \simeq e^{-i k_o \mathfrak{z} + \pi i \lambda \mathfrak{z} (u^2 + v^2)} \tag{7}$$

$$(k_o \approx 2\pi / \lambda)$$

and one obtains then

$$\gamma_{\mathfrak{z}}(\bar{x}) = \overline{\mathcal{F}} \left[\Gamma_{\mathfrak{z}}(\bar{u}) \right] = i \frac{e^{-i k_o \mathfrak{z}}}{\lambda \mathfrak{z}} g_{\mathfrak{z}}(\bar{x}) \tag{8}$$

with

$$g_{\mathfrak{z}}(\bar{x}) = e^{-\pi i \frac{x^2 + y^2}{\lambda \mathfrak{z}}} = e^{-\pi i \frac{\bar{x}^2}{\lambda \mathfrak{z}}} \tag{9}$$

The function $\gamma_{\mathfrak{z}}(\bar{x})$ is named Fresnel function and the convolution
product by $\gamma_{\mathfrak{z}}$ a Fresnel-transform [15]:

$$Fr_{\mathfrak{z}} \left[f(\bar{x}) \right] = f(\bar{x}) * \gamma_{\mathfrak{z}}(\bar{x}) \tag{10}$$

After (5), the remote field is then obtained by a Fresnel transform of the aperture field.

A3) Properties of the Fresnel Transform

The relationship

$$\int_{-\infty}^{+\infty} e^{\pi i \frac{x^2}{\lambda z}} \, f(x) \, e^{-\pi i \frac{(x-x_0)^2}{\lambda z}} \, dx = \int_{-\infty}^{+\infty} f(x) \, e^{2\pi i \frac{x x_0}{\lambda z} - \pi i \frac{x_0^2}{\lambda z}} \, dx$$

may be written:

$$g_z^*(\bar{x}) \, f(\bar{x}) * g_z(\bar{x}) = g_z(\bar{x}_0) \, \mathcal{F}_{\frac{\bar{x}_0}{\lambda z}} \left[f(\bar{x}) \right]$$

or

$$F_z \left[f(\bar{x}) \right] = i \, \frac{e^{-i k_0 z}}{\lambda z} \, g_z(\bar{x}_0) \, \mathcal{F}_{\frac{\bar{x}_0}{\lambda z}} \left[f(\bar{x}) \, g_z(\bar{x}) \right] \qquad (11)$$

a useful relationship between Fresnel and F.T. [15, 16].

We shall also quote the following relationships:

$$g_{z_1}(\bar{x}) \cdot g_{z_2}(\bar{x}) = g_{\frac{z_1+z_2}{z_1 \cdot z_2}}(\bar{x}) \qquad (12)$$

and

$$\gamma_{z_1}(\bar{x}) * \gamma_{z_2}(\bar{x}) = \gamma_{z_1+z_2}(\bar{x}) \qquad (13)$$

$$\gamma_z(\bar{x}) * \gamma_{-z}(\bar{x}) = \delta(\bar{x}) \qquad (14)$$

After (5) and (14), we verify that

$$Fr_{\substack{3=0}} \left[E(\bar{x}) \right] = E(\bar{x}) * \delta(\bar{x}) = E(\bar{x})$$

and after (11)

$$Fr_{3 \to \infty} \left[E(\bar{x}) \right] = \frac{i e^{-i k_0 3}}{\lambda 3} g_\infty(\bar{x}) \, \mathcal{F}_{\frac{\bar{x}}{\lambda 3}} \left[E(\bar{x}) . g_\infty(\bar{x}) \right]$$

$$= \frac{i e^{-i k_0 3}}{\lambda 3} \, \mathcal{F}_{\frac{\bar{x}}{\lambda 3}} \left[E(\bar{x}) \right]$$

(The far-zone distribution is proportional to the F.T. of the aperture distribution)

A4) Function of a lens

We shall describe the function of a lens by a pure multiplication of the field on its entrance face by a quadratic phase factor:

$$\phi(\bar{x}) = g_f^*(\bar{x}) \tag{15}$$

A pupil function may be superimposed on this phase factor to describe the finite dimension of the lens.

A5) Imaging

Let E_{η_1} be a given field distribution in the plane η_1.
An aperture with a given pupil function $P(\bar{a})$ is placed in the plane a at the distance d_1, of η_1. We wish to calculate the distribution $E_{\eta_2}(\bar{\xi})$ in the plane η_2 placed at the distance d_2 from a.
Using (11)

$$E_a(\bar{a}) = Fr_{d_1} \left[E_{\eta_1}(\bar{x}) \right] = \gamma_{d_1}(\bar{a}) \, \mathcal{F}_{\frac{\bar{a}}{\lambda d_1}} \left[E_{\eta_1}(\bar{x}) g_{d_1}(\bar{x}) \right]$$

Multiplying by $P(\bar{\alpha})$ and making once again a Fresnel transform to carry the field to the plane π_2 :

$$E_{\pi_2}(\bar{\xi}) = - \frac{e^{-ik_o(d_1+d_2)}}{\lambda^2 d_1 d_2} \; g_{d_2}(\bar{\xi}) \; \underset{\frac{\bar{\xi}}{\lambda d_2}}{\mathcal{F}} \left\{ g_{d_2}(\bar{\alpha}) P(\bar{\alpha}) g_{d_1}(\bar{\alpha}) \underset{\frac{\bar{\alpha}}{\lambda d_1}}{\mathcal{F}} \left[E_{\pi_1}(\bar{x}) g_{d_1}(\bar{x}) \right] \right\} \quad (16)$$

It may be advantageous to write the F.T. in (16) under the form of a convolution product, which yields:

$$E_{\pi_2}(\bar{\xi}) = - \frac{e^{-ik_o(d_1+d_2)}}{\lambda^2 d_1 d_2} \; g_{d_2}(\bar{\xi}) \left\{ \vphantom{\frac{d_1}{d_2}} \right.$$

$$\left. \left\{ E_{\pi_1}(-\bar{\xi}\frac{d_1}{d_2}) \; g_{d_1}(-\bar{\xi}\frac{d_1}{d_2}) * \underset{\frac{\bar{\xi}}{\lambda d_2}}{\mathcal{F}} \left[P(\bar{\alpha}) g_{d_1}(\bar{\alpha}) g_{d_2}(\bar{\alpha}) \right] \right\} \right\} \quad (17)$$

A6) Image given by a lens

Using the relationship (17) with

$$P(\bar{\alpha}) = P_o(\bar{\alpha}) \cdot g_f^*(\bar{\alpha})$$

in which $P_o(\bar{\alpha})$ is a diaphragm function, g_f^* the lens function, and $1/d_1 + 1/d_2 = 1/f$, we get, taking account of

$$g_{d_1} \cdot g_{d_2} = g_f \qquad \text{and} \qquad g_f g_f^* = 1$$

$$E_{\pi_2}(\bar{\xi}) = - \frac{e^{-ik_o(d_1+d_2)}}{\lambda^2 d_1 d_2} \; g_{d_2}(\bar{\xi}) \left\{ \cdots \vphantom{\frac{d_1}{d_2}} \right.$$

$$\left. \left\{ E_{\pi_1}(-\bar{\xi}\frac{d_1}{d_2}) \; g_{d_1}(-\bar{\xi}\frac{d_1}{d_2}) * \tilde{P}_o(\frac{\bar{\xi}}{\lambda d_2}) \right\} \right\} \quad (18)$$

where $\tilde{P}_o(\bar{\xi}/\lambda d_2) = \underset{\bar{\xi}/\lambda d_2}{\mathcal{F}}[P_o(\bar{\alpha})]$ is the usual diffraction pattern of the lens aperture.

Even for a perfect and infinitely extended lens, the image distribution is not exactly the magnified object but is affected

by a phase factor $g_{d_2}(\bar{\xi}) \cdot g_{d_1}(-\bar{\xi}\,\frac{d_1}{d_2})$. (In coherent imaging
a lens is not a perfectly linear device [17]. It should be
mentioned that this "error" may be compensated by a judicious
choice of the illuminating wave as shown in ref.[18].)

A7) Back focal plane distribution

Placing now the object distribution in the focal plane in
front of the lens, we calculate the distribution in the back
focal plane.

In this case $\quad d_1 = d_2 = f$

$$P = P_0\, g_f^*$$

The formula (17) reads now:

$$E_{n_2}(\bar{\xi}) = \frac{-e^{-2ikf}}{\lambda^2 f^2}\ g_f(\bar{\xi}) \left\{ E_{n_1}(-\bar{\xi})\,g_f(-\bar{\xi}) * \mathcal{F}_{\frac{\bar{\xi}}{\lambda d_2}}\left[P_0(\bar{\alpha})\,g_f(\bar{\alpha}) \right] \right\} \quad (19)$$

Now using (7) and (8)

$$\mathcal{F}_{\frac{\bar{\xi}}{\lambda f}}\left[P_0(\bar{\alpha})\, g_f(\bar{\alpha}) \right] = \widetilde{P}_0\left(\frac{\bar{\xi}}{\lambda f}\right) \underset{\bar{\xi}/\lambda f}{*} \mathcal{F}_{\frac{\bar{\xi}}{\lambda f}}\left[g_f(\bar{\alpha}) \right]$$

$$= \widetilde{P}_0\left(\frac{\bar{\xi}}{\lambda f}\right) \underset{\bar{\xi}/\lambda f}{*} \left[-i\lambda f\, e^{ikf}\, \Gamma_f\left(\frac{\bar{\xi}}{\lambda f}\right) \right]$$

$$= \widetilde{P}_0\left(\frac{\bar{\xi}}{\lambda f}\right) \underset{\bar{\xi}}{*} \left[-\frac{i}{\lambda f}\, g_f^*(\bar{\xi}) \right]$$

where the integration variable for the convolution is shown
under the star.
Putting this result in the equation (19) above and using the
associativity of the convolution product [19] we get first:

$$E_{n_1}(-\bar{\xi})\,g_f(-\bar{\xi}) * g_f^*(\bar{\xi}) = g_f^*(\bar{\xi})\, \mathcal{F}_{\frac{\bar{\xi}}{\lambda f}}\left[E_{n_1}(\bar{\xi}) \right]$$

as follows from (11)
and finally:

$$E_{\eta_2} = \frac{i \, e^{-2ik_o f}}{\lambda^3 \rho^3} \; g_\rho(\bar{\xi}) \left\{ g_f^*(\bar{\xi}) \; \widetilde{E}(\tfrac{\bar{\bar{\xi}}}{\lambda f}) \; \ast \; \widetilde{P}_o(\tfrac{\bar{\xi}}{\lambda f}) \right\} \qquad (21)$$

For a perfect and infinitely wide lens:

$$\widetilde{P}_o(\tfrac{\bar{\xi}}{\lambda f}) = \delta(\tfrac{\bar{\xi}}{\lambda f}) = \lambda^2 \rho^2 \, \delta(\bar{\xi})$$

$$E_{\eta_2}(\bar{\xi}) = \frac{i \, e^{-2ik_o f}}{\lambda f} \; \widetilde{E}_{\eta_1}(\tfrac{\bar{\xi}}{\lambda \rho}) \qquad (22)$$

The distribution in the back focal plane is then the F.T. of
this in the front focal plane, a well-known result whose
physical meaning is readily apparent when one considers a
plane wave (a "Fourier" component of E_{η_1}) impinging on the
lens: its "image" in the back focal plane is a single point.

The two first factors in (21) cancel out exactly for a
perfect lens. Let us now see what they become in an actual
situation. To do this, we shall compare the actual distribution
given above and which may be rewritten as:

$$E_{\eta_2}(\bar{\xi}) = \kappa \iint g_\rho(\bar{\xi}) \, g_f^*(\bar{r}) \, \widetilde{E}(\tfrac{\bar{r}}{\lambda f}) \, P_o(\tfrac{\bar{\xi}-\bar{r}}{\lambda f}) \, d\bar{r} \qquad (23)$$

with another distribution

$$E'_{\eta_2}(\bar{\xi}) = \kappa \; \widetilde{E}(\tfrac{\bar{\xi}}{\lambda f}) \underset{\bar{\xi}}{\ast} P_o(\tfrac{\bar{\xi}}{\lambda f}) = \kappa \iint \widetilde{E}(\tfrac{\bar{r}}{\lambda f}) \, \widetilde{P}_o(\tfrac{\bar{\xi}-\bar{r}}{\lambda f}) d\bar{r} \qquad (24)$$

The actual result (23) is not a convolution product, but taking
account of the fact that $P_o(\tfrac{\bar{\xi}-\bar{r}}{\lambda f})$ (the diffraction pattern of the
aperture) is a narrow function of $\bar{\xi}-\bar{r}$ of width $\Delta(\bar{\xi}-\bar{r}) = 2\tfrac{\lambda \rho}{A}$
(A is the aperture diameter).
We see that the total phase variation introduced by $g_\rho(\bar{\xi}) \, g_f^*(\bar{r})$

over the width of the diffraction pattern is at most

$2\pi \dfrac{\xi_M + \gamma_M}{A} \simeq 2\pi$, where ξ_M and γ_M are the greatest vector radii of the object and the image respectively and each of the order of $A/2$.

Now, consider a point $\bar{\xi}_0$ in the π_2 plane; in the ideal case (eq.22) it bears information only on one Fourier component of E_{π_1}. In the "half ideal" case of eq.(24) the neighbouring points of the spectrum contribute also to the illumination in $\bar{\xi}_0$. In the actual case (eq.23) the smearing effect due to the finite width of $\widetilde{P}_0$ is reduced (if the spectrum $\widetilde{E}$ is smooth enough) because the contributions in the integral of two neighbouring points, symmetrically placed with regard to $\bar{\xi}_0$ appear now with opposite phases, and then partly cancel out. Thus, the actual diffraction effects should be less severe as those predicted by the simple equation (24) which will then be accepted as a good approximation for the points of π_2 near the optic axis, hence consistent with the paraxial approximation. (Away from the axis, the cancellation is even more effective.)

Therefore, we shall use the following approximation:

$$E_{\pi_2}(\bar{\xi}) = \frac{i\, e^{-2ik_0 f}}{\lambda^3 \rho^3} \left[\widetilde{E}_{\pi_1}(\tfrac{\bar{\xi}}{\lambda f}) \underset{\bar{\xi}}{*} \widetilde{P}_0(\tfrac{\bar{\xi}}{\lambda f}) \right] \qquad (25)$$

It should be noticed here that this approximation gives rise to an important feature which becomes apparent if we replace the convolution product of F.T. above by the F.T. of the product:

$$E_{\pi_2}(\bar{\xi}) = K \mathcal{F}_{\bar{\xi}/\lambda\rho} \left[E_{\pi_1}(\bar{\xi}) \cdot P_0(\bar{\xi}) \right]$$

This shows that the diaphragm function P, acts as a mask placed in the plane of the object. This is not in contradiction with the usual conception of the diaphragm as a limiter for the spectrum because the distribution E_{π_1} is indeed a spectrum whose image is given by the lens.

Back-focal plane "image" of the aperture distribution:

The object distribution is now placed on the entrance face of the lens. We calculate the back focal plane distribution:

$$E_{\eta 2}(\bar{\xi}) = \frac{i e^{-ik_o \rho}}{\lambda^3 \rho^3} \, g^{(\bar{\xi})}_\rho \left[\widetilde{E}_{\eta 1}(\frac{\bar{\xi}}{\lambda \rho}) \underset{\bar{\xi}}{*} \widetilde{P}_o(\frac{\bar{\xi}}{\lambda \rho}) \right]$$

$$= \mathcal{F}r_\rho \left[g_\rho^*(\bar{\alpha}) \, E_{\eta 1}(\bar{\alpha}) \, P_o(\bar{\alpha}) \right] \qquad (26)$$

Here again, information on the F.T. of the object distribution may be retrieved in the back-focal plane, a property which we use in one of the devices of table I (1.1).

As a special case, the use of a delta function $A(\bar{\alpha}_o)\,\delta(\bar{\alpha}-\bar{\alpha}_o)$ as object results in an image:

$$E_{\eta 2}(\bar{\xi}) = \frac{i e^{-ik_o \rho}}{\lambda \rho} \, g_\rho(\bar{\xi}) \, e^{2\pi i \, \bar{\xi}\bar{\alpha}_o / \lambda \rho} \, P_o(\bar{\xi}) \, A(\alpha_o)$$

and for $\bar{\xi} = 0$ (for a receiver on axis)

$$E_{\eta 2}(\bar{\xi}) = \frac{i e^{-ik_o \rho}}{\lambda \rho} \, P_o(\bar{\alpha}_o) \, A(\bar{\alpha}_o) \qquad (27)$$

A8) Fourier plane filtering

We study now the system of fig. 2 corresponding to the actual configuration of the MISS. Introducing a pupil function $Q(\bar{\xi})$ in the plane π_2 , we may write from the preceding section:

$$E_{\eta 2}(\bar{\xi}) = \frac{i e^{-2ik_o \rho_1}}{\lambda^3 \rho_1^3} \left[\widetilde{E}_{\eta 1}(\frac{\bar{\xi}}{\lambda \rho_1}) \underset{\bar{\xi}}{*} \widetilde{P}_1(\frac{\bar{\xi}}{\lambda \rho_1}) \right] Q(\bar{\xi}) \qquad (28)$$

The transformation from the plane π_2 to the plane π_3 is the same as from π_1 to π_2 , so that

$$E_{\eta 3}(\bar{x}) = -\frac{e^{-2ik_o(\rho_1+\rho_2)}}{\lambda^6 \rho_1^3 \rho_2^3} \left\{ \underset{\frac{\bar{x}}{\lambda \rho_2}}{\mathcal{F}} \left[Q(\bar{\xi}) \left(\widetilde{E}_{\eta 1}(\frac{\bar{\xi}}{\lambda \rho_1}) \underset{\bar{\xi}}{*} \widetilde{P}_1(\frac{\bar{\xi}}{\lambda \rho_1}) \right) \right] \widetilde{P}_2(\frac{\bar{x}}{\lambda \rho_2}) \right\} \qquad (29)$$

using

$$\underset{\bar{x}/\lambda \rho_2}{\mathcal{F}} \left[\widetilde{E}_{\eta 1}(\frac{\bar{\xi}}{\lambda \rho_1}) \right] = \lambda^2 \rho_1^2 \, E_{\eta 1}(-\bar{x} \frac{\rho_1}{\rho_2})$$

$$E_{\eta 3}(\bar{x}) = -\frac{e^{-2ik_o(\rho_1+\rho_2)}}{\lambda^4 \rho_1 \rho_2^3} \left\{ \widetilde{Q}(\frac{\bar{x}}{\lambda \rho_2}) \underset{\bar{x}}{*} \left[P_1(-\frac{\bar{x}\rho_1}{\rho_2}) \cdot E_{\eta 1}(-\bar{x}\frac{\rho_1}{\rho_2}) \right] \underset{\bar{x}}{*} \widetilde{P}_2(\frac{\bar{x}}{\lambda \rho_2}) \right\} \qquad (30)$$

We see that the function P_1 plays the role of a diaphragm placed

in the object plane. This results from our approximation of section A7). In particular, P_1 introduces a field limitation in the object plane.

We shall now drop the term P_1, bearing in mind its meaning.

The overall pupil function of the device may now be written

$$\widetilde{D}(\bar{x}) = \widetilde{Q}(\frac{\bar{x}}{\lambda f_2}) \underset{\bar{x}}{*} \widetilde{P}_2(\frac{\bar{x}}{\lambda f_2}) \tag{31}$$

Its reverse F.T.

$$D(\frac{\bar{\xi}}{\lambda f_2}) = \lambda^4 f_2^4 \; Q(\bar{\xi}) \cdot P_2(\bar{\xi}) \tag{32}$$

The second pupil function P_2 plays the role of a mask in the Fourier plane, i.e. the same role with regard to the F.T. of the object as this of P_1, with regard to the object itself as could be expected.

As for P_1, we shall now also drop this term to alleviate the notations.
We become then

$$E_{n_2}(\bar{x}) = - \frac{e^{-2ik_0(f_1+f_2)}}{\lambda^2 f_1 f_2} \; \widetilde{Q}(\frac{\bar{x}}{\lambda f_2}) \underset{\bar{x}}{*} E_{n_1}(-\bar{x}\frac{f_1}{f_2}) \tag{33}$$

For a perfect pupil function Q,

$$E_{n_2}(\bar{x}) = - \frac{f_1}{f_2} e^{-2ik(f_1+f_2)} E_{n_1}(-\bar{x}\frac{f_1}{f_2}) \tag{34}$$

A9) Pupil functions

We consider different pupil functions and the associated diffraction patterns.

1) Aperture function

$$Q_1(\bar{x}) = \begin{array}{ll} 1 & \text{for } |x| < A, \; |y| < B \\ 0 & \text{for } |x| \geqslant A, \; |y| \geqslant B \end{array} \tag{35a}$$

which yields:

$$\widetilde{Q}_1(\bar{u}) = 4AB \frac{\sin 2\pi Au}{2\pi Au} \cdot \frac{\sin 2\pi Bv}{2\pi Bv} \tag{35b}$$

2) Finite array of equidistant points:

$$Q_2(\bar{x}) = ab \sum_{n=-N}^{+N} \sum_{m=-M}^{M} \delta(x-na, y-mb) \tag{36a}$$

$$\widetilde{Q}_2(\bar{u}) = ab \sum_{n=-N}^{N} \sum_{m=-M}^{M} e^{2\pi i(nau+mbv)}$$

which may also be written:

$$\widetilde{Q}_2(\bar{u}) = ab \frac{\sin(2N+1)\pi au}{\sin \pi au} \frac{\sin(2M+1)\pi bv}{\sin \pi bv}$$

(the usual array diffraction pattern)
letting now

$$\widetilde{Q}_2'(\bar{u}) = \widetilde{Q}_2(\bar{u}) \quad \text{for} \quad |u| < \frac{1}{2a}, |v| < \frac{1}{2b}$$

$$= 0 \qquad \text{outside}$$

we get:

$$\widetilde{Q}_2 = \widetilde{Q}_2'(\bar{u}) * \sum_{n=-\infty}^{\infty} \sum_{m=-\infty}^{\infty} \delta(u-\frac{n}{a}, v-\frac{m}{b}) \tag{36b}$$

where the summation has been limited to orders which give rise to actual images, i.e. so that

$$\infty \leqslant \frac{a}{\lambda} \quad , \quad \infty \leqslant \frac{b}{\lambda}$$

3) Phase modulating aperture

$$Q_3(\bar{x}) = e^{2\pi i(\alpha\frac{x}{a} + \beta\frac{y}{b})} \tag{39a}$$

$$\widetilde{Q}_3(\bar{u}) = \delta(u-\frac{\alpha}{a}, v-\frac{\beta}{b}) \tag{39b}$$

4) Zoned aperture

$$Q_4(\bar{x}) = S\left[\cos(\phi_0 + 2\pi\alpha\frac{x}{a})\right] \cdot S\left[\cos(\psi_0 + 2\pi\beta\frac{y}{b})\right]$$

where $S(y) = 1$ for $y > 0$

$\qquad\qquad = 0$ for $y \leq 0$ (40a)

$$\tilde{Q}_4(\bar{u}) = \sum_{k=-\infty}^{+\infty} \sum_{l=-\infty}^{+\infty} \frac{e^{-ik\phi_0} \sin k\pi/2}{k\pi} \frac{e^{-il\psi_0} \sin l\pi/2}{l\pi} \cdot$$

(40b)

$$\cdot \delta(u - \frac{k\alpha}{a}) \delta(v - \frac{l\beta}{b})$$

5) Array of phase modulating scatterers:

$$Q_5(\bar{x}) = Q_2(\bar{x}) \cdot Q_3(\bar{x})$$ (37a)

$$\tilde{Q}_5(\bar{u}) = Q_2(\bar{u}) * \sum_{-\infty}^{\infty} \sum_{-\infty}^{\infty} \delta(u - \frac{n+\alpha}{a}) \cdot$$

$$\cdot \delta(v - \frac{m+\beta}{b})$$

(37b)

6) Array of modulating diodes

$$Q_6(\bar{x}) = Q_2(\bar{x}) \cdot Q_4(\bar{x})$$ (38a)

$$\tilde{Q}_6(\bar{u}) = \tilde{Q}'_2(\bar{u}) * \left\{ \sum_{n=-\infty}^{\infty} \sum_{k=-\infty}^{+\infty} \frac{e^{-ik\phi_0} \sin k\pi/2}{k\pi} \delta(u - \frac{k\alpha+n}{a}) \cdot \right.$$

$$\left. \cdot \sum_{m=-\infty}^{\infty} \sum_{l=-\infty}^{+\infty} \frac{e^{-il\psi_0} \sin l\pi/2}{l\pi} \delta(v - \frac{l\beta+m}{b}) \right\}$$

(38b)

A10) The correspondence object image in the Microwave Image Scanning System:

We summarize here the results obtained for the system of fig. 2: a modulated scattering array placed in the Fourier plane of an afocal system.

The array is constituted by $(2N_x+1)(2N_y+1)$ scattering points (distance between two rows = a; between two columns = b). The scatterer placed at the point x, y is modulated by a square wave:

$$S\left[\cos\left[(\Omega t + \varphi_o + \delta\Omega t \tfrac{x}{a})\right]\right] \cdot S\left[\cos\left(\omega t + \psi_o + \delta\omega t \tfrac{y}{b}\right)\right]$$

where $S(y)$ stands for
$$\begin{cases} 1 \text{ if } y \geqslant 0 \\ 0 \text{ if } y < 0 \end{cases}$$

The (modulated) image given by the system consists in a double multiplicity of images: each image given by the non modulated array (indexed by n, m with $n \leqslant \mathcal{K} = \tfrac{a}{\lambda}$, $m \leqslant \mathcal{K} = \tfrac{b}{\lambda}$) is split under the effect of modulation into a set of travelling images (k, l) each moving in the image plane with velocity components proportional to (k, l). One of these sub-images (m, n; k, l) shows an amplitude distribution: using (33, 36b, 38b):

$$e_{n2}(n,m,k,\ell)(\bar{x}) = \frac{-ab\, e^{-2ik_o(f_1+f_2)}}{\lambda^2 f_1 f_2} \frac{e^{-i(k\Omega + l\omega)t}}{kl\pi^2} \sin\tfrac{k\pi}{2} \sin\tfrac{l\pi}{2} \cdot$$

$$\cdot \left\{ E_{n1}\left(-\kappa\tfrac{f_1}{f_2}\right) \underset{x_o y_o}{*} \frac{\sin(2N_x+1)\pi\frac{ax_o}{\lambda f_2}}{\sin \pi a x/\lambda f_2} \cdot \frac{\sin(2N_y+1)\pi\frac{by_o}{\lambda f_2}}{\sin \pi b y/\lambda f_2} \right\}$$

$$\tag{41}$$

$$x_o = x + \left(n + \frac{k\,\delta\Omega \cdot t}{2\pi}\right)\frac{\lambda f_2}{a} \quad; \quad y_o = y + \left(m + \frac{\ell\,\delta\omega t}{2\pi}\right)\frac{\lambda f_2}{b}$$

where

a sub-image is then the initial distribution convolved with the usual array diffraction pattern and translated by an amount

$$\begin{cases} \Delta x = -\left(n + \frac{k\,\delta\Omega \cdot t}{2\pi}\right)\frac{\lambda f_2}{a} \\ \\ \Delta y = -\left(m + \frac{\ell\,\delta\omega t}{2\pi}\right)\frac{\lambda f_2}{b} \end{cases}$$

$$\tag{42}$$

It should be noticed that practically no loss of resolution is introduced with regard to the steady image given by the optical system (except for the replacement of the aperture pattern [35b] , by this of the array:[36b].

Acknowledgement

References

[1] J. Brown   Proc.IEE 105C, p.343 (1958)

[2] J.G.Wegrowe   Thèse Paris 1963 "Interferométre microonde
                         à optique focalisante pour le diagnostic
                         des plasmas"

[3] R. Justice   IRE Trans. AP3, 177 (1955)
     V.H.Rumsey

[4] A.L. Cullen   Proc.IEE 102B, p.836 (1955)
     J.C.Parr

[5] Ming-Kuei-Hu   IRE Trans.MTT, p. 295 (1960)

[6] P.A.Matthews   Proc.IEE 103-C (1956)
     A.L. Cullen   "A study of the field distribution at an
                         axial focus of a square microwave lens"

[7] K. Iizuka   Electronics 15 April 1968, p.130
                                     24 June 1968 p.122

[8] J.A.Zinoviev   Sov.Physics JETP 25, 752 (1967)

[9] C.F.Augustine   Electronics 24.6, 118 (1968)

[10] C.F.Augustine   "Microwave" (to be published)
                         "Real time area detection ofelectromagnetic
                         fields using cholesteric liquid crystals"

[11] H.Jacobs   Journ.Opt.Soc.Am.58, 246 (1968)
     R.Hofer
     G.Morris
     E.Horn

[12] R.Whitmann   Symp.on Modern Optics, Polyt.Press N.Y.
     A.Korpel   1967, p. 243
     S.Lotsoff

[13] M. Arm et.al.   Symp.on Modern Optics, Polyt.Press N.Y.
                         (1967) p. 691

[14] P.C. Clemmow   Perg.Press (1966) "The plane wave spectrum
                         representation of electromagnetic fields"

[15] L. Mertz   "Transformations in Optics" John Wiley (1965)

[16] V.S. Auerbach   in "Electromagnetic wave theory" J.Brown ed.,
     S.N. Vlasov   Pergamon Press (1965), p.445
     V.I. Talanov

[17] P. Dumontet   in "Astronomical Optics" North-Holland
                   Publ.Comp. (1956), p.93 "La correspondance
                   objet-image en optique"

[18] S. Lowenthal Optica Acta 12, 261 (1965)

[19] J. Arsac   Dunod, Paris 1961 "Transformation de
                   Fourier et theorie des distributions"

Figure Captions

Fig. 1   Different systems used to measure microwave field
                distributions

Fig. 2   Disposition of the optical set-up used in MISS
                (array placed in the plane Π_2)
                Notations

Fig. 3   Imaging: transformation from the object plane Π_1,
                to the image plane Π_3 by means of different pupil
                functions placed in the Fourier plane Π_2 ;
                successively:
                - Unlimited aperture
                - limited aperture
                - unlimited phase modulation (point object, then
                  extended object)
                - sampled unlimited phase modulation (point object,
                  then extended object)

Fig. 4   Disposition and feeding of an array of diodes

Fig. 5   "Spatial biasing" of the receiver:
                images of different orders n for $\delta\Omega.t = 0$
                $\delta\Omega.t \neq 0$ displacement whith time of the images of
                different orders n and different carrier frequency
                $\delta\Omega.t = \Pi$: limitation of the available field
                to $\lambda f/2a$ due to the beginning of overlapping of
                the images $(n = 0,\ k = 1)$ and $(n = 1,\ k = -1)$

Fig. 6   Field distribution measurements at $\lambda = 8.6\ mm$
                image given by a dielectric lens (diameter 20 cm,
                f = 10 cm) of an open waveguide

Fig. 7   Point to point measurement (the array is placed in
                the image plane - same set-up as in fig. 6)

Fig. 8   Block diagram of the set-up used for the
measurement of fig. 9

Fig. 9   Measurement with MISS (the array is placed in
the Fourier plane Π_2 of fig. 2):
Unidimensional explorations with an array of 5x5
diodes placed 1 cm apart from each other
(λ = 8,6 mm - f = 10 cm)

unknown distribution

P

E

R

direct measurement

P

E

S

R

measurement by scattering

P

R

E

S

measurement by scattering and using the reciprocity

E

L

L

R

through an optical system

P
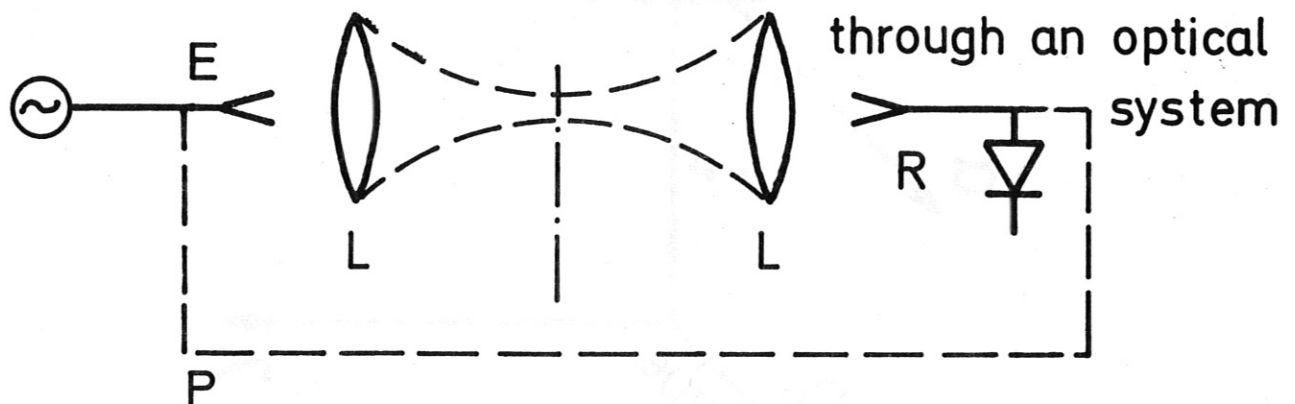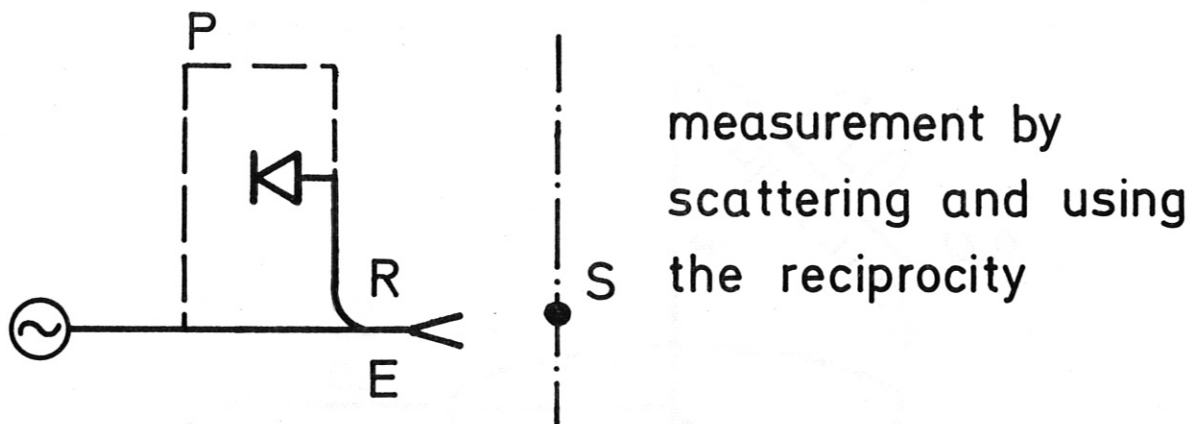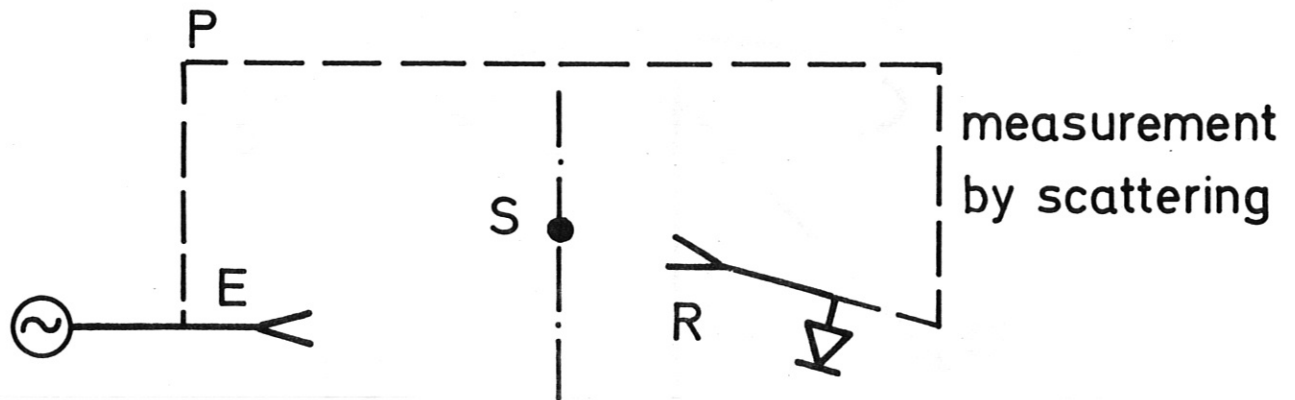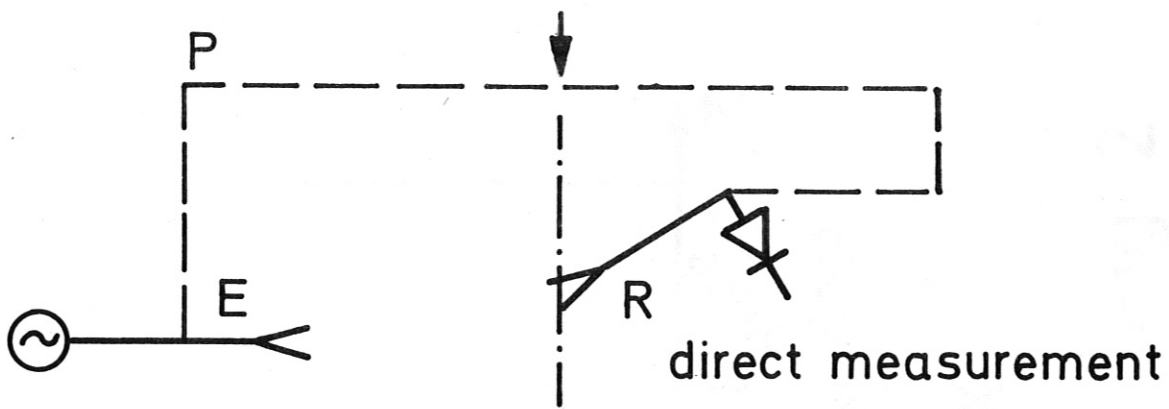
E   emitter   R   receiver
S   scatterer   L   lens
P   reference path for phase measurement

Fig. 1

Fig. 2

Imaging

Plane (Π_1)	Plane (Π_2)	Plane (Π_3)

Fig. 3

$V_0 \cos(\Omega + \delta\Omega)t$ $V_0 \cos \Omega t$ $V_0 \cos(\Omega - \delta\Omega)t$

$n_x =$ +2 +1 0 -1 -2

$n_y =$

$V_0 \cos(\omega + 2\delta\omega)t$ +2

$V_0 \cos(\omega + \delta\omega)t$ +1

$V_0 \cos \omega t$ 0

$V_0 \cos(\omega - \delta\omega)t$ -1

$V_0 \cos(\omega - 2\delta\omega)t$ -2

b

a
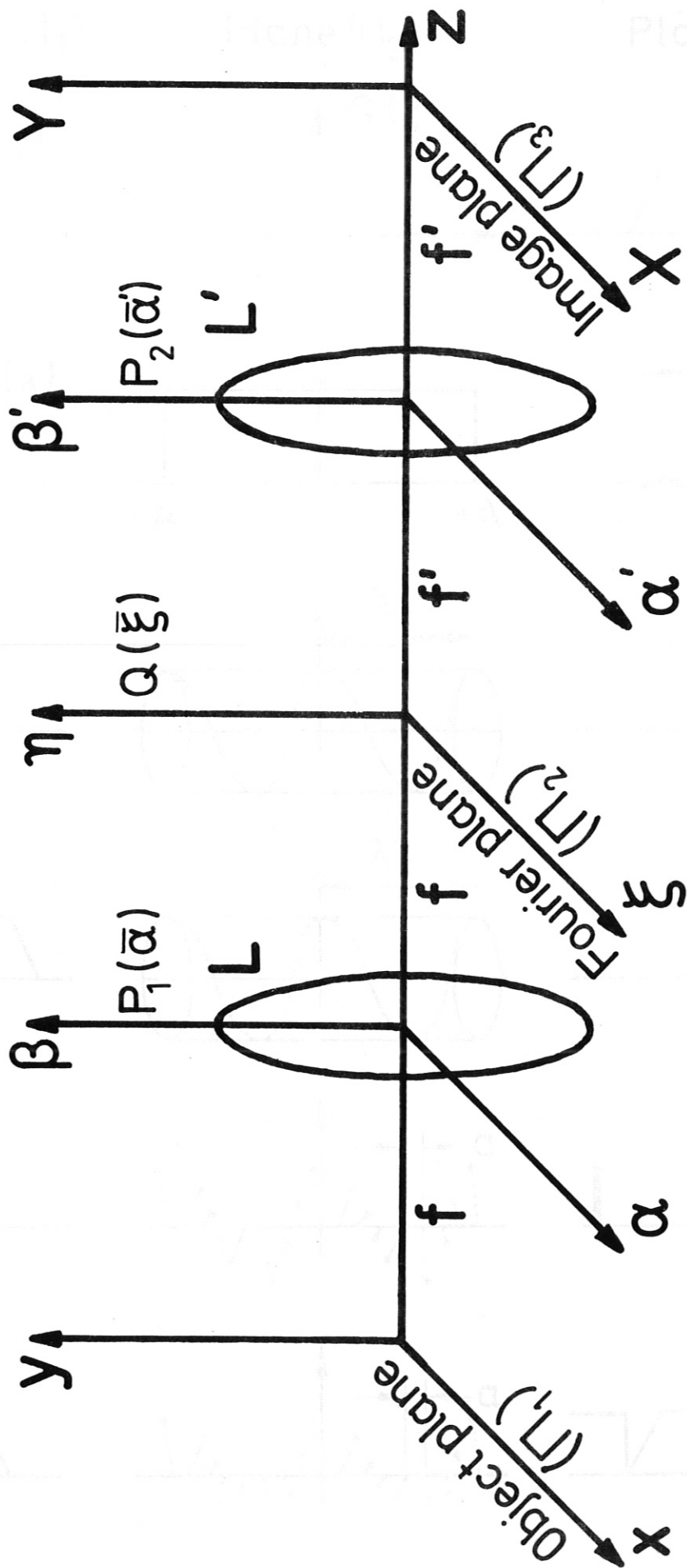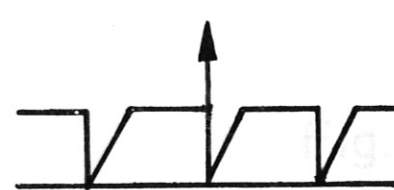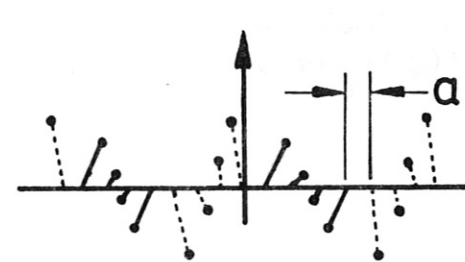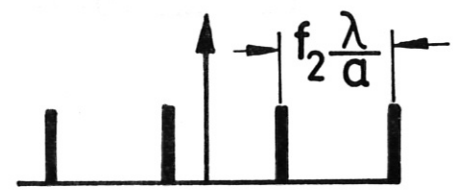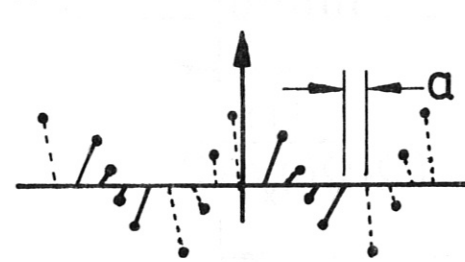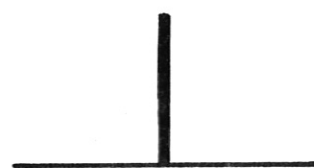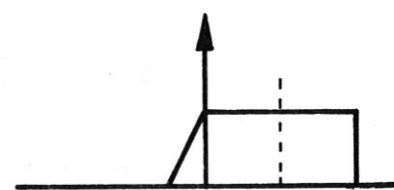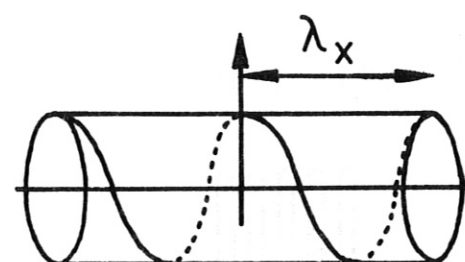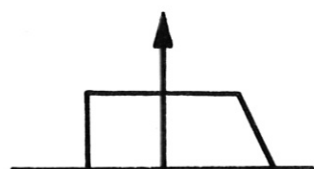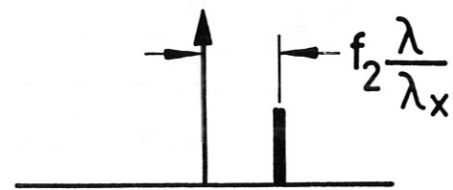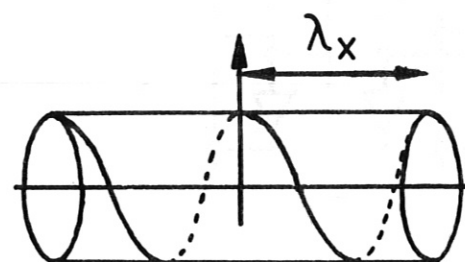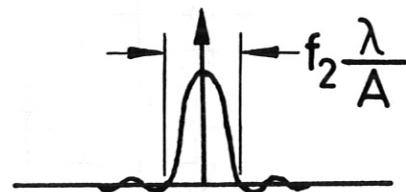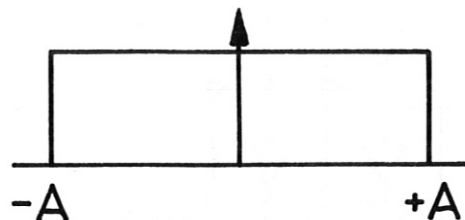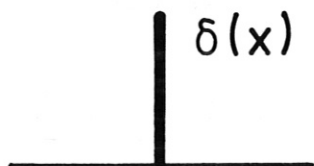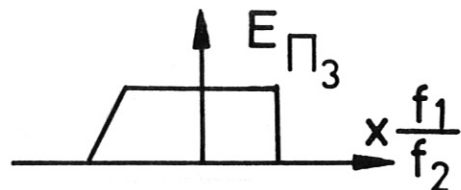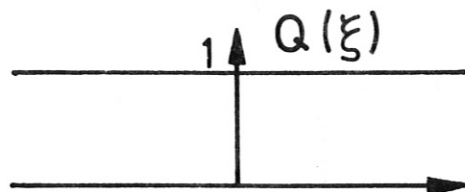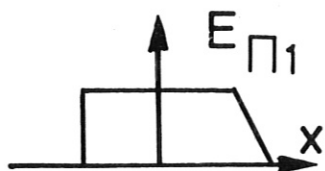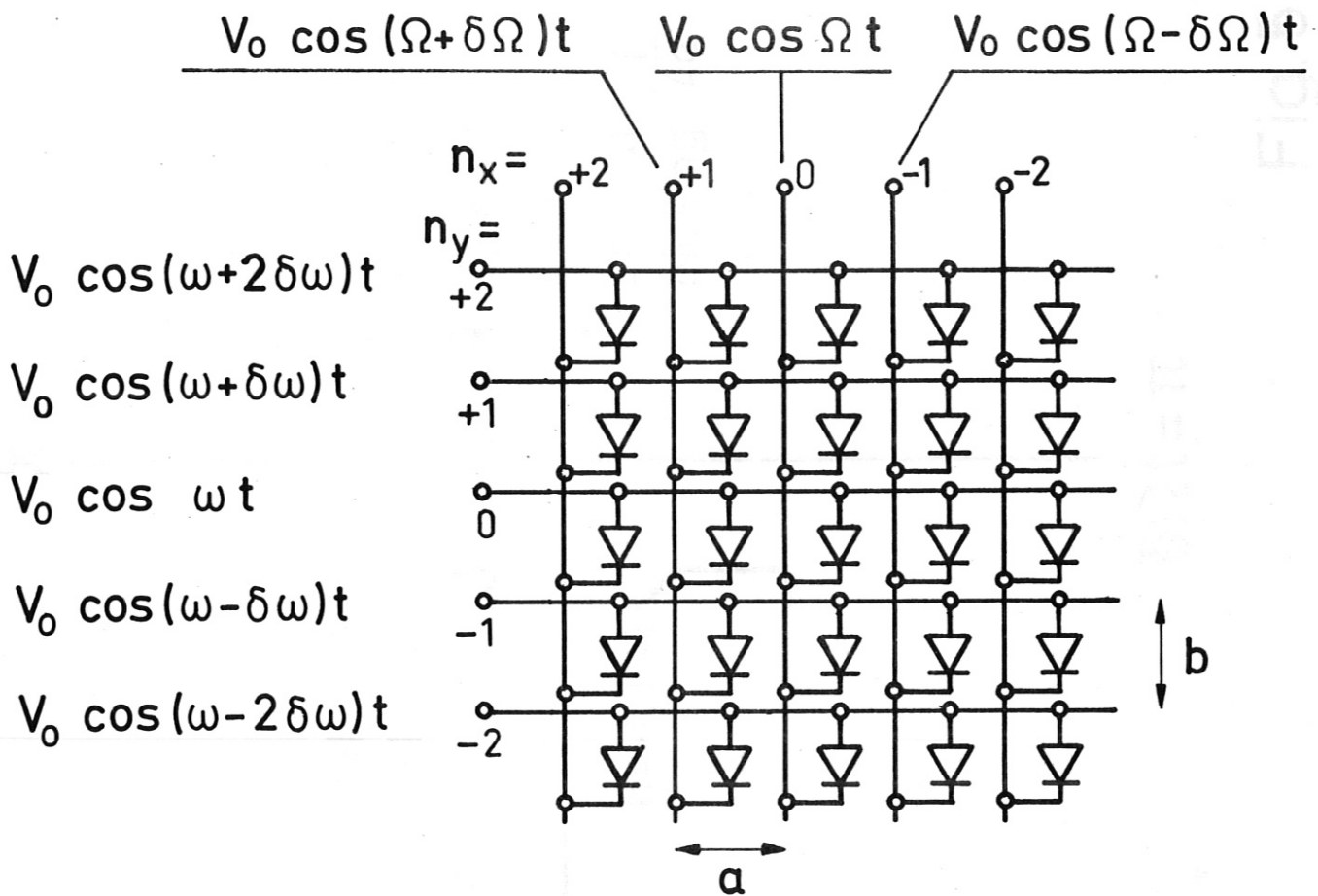
Current in the diode $n_x \, n_y$

$$\frac{2\Pi}{\Omega + n_x(\delta\Omega + \Omega)}$$

$$\frac{2\Pi}{\omega + n_y(\delta\omega + \omega)}$$

Fig. 4

Images

$\delta\Omega t = 0$

$\delta\Omega t = \pi/4$

$\delta\Omega t = \pi$

Spatial biasing

Fig. 5

Receiver

Optic axis

$n=1$

$n=0$

$n=-1$

$\frac{\lambda f}{a}$

$k=1$

$k=-1$

$k=1$

$k=-1$

$k=1$

$k=-1$

R

$n=1, k=-1$
$n=0, k=1$

$n=-1, k=1$

R

Field limitation:

$D_x = \frac{\lambda f}{2a}$
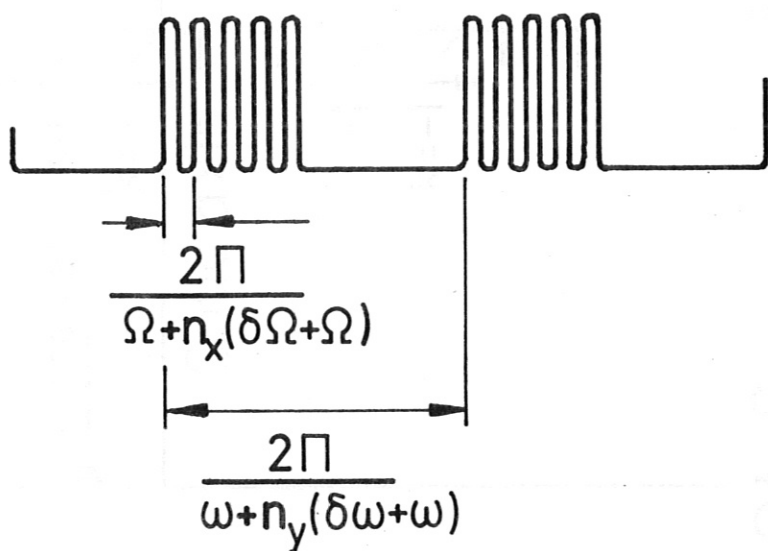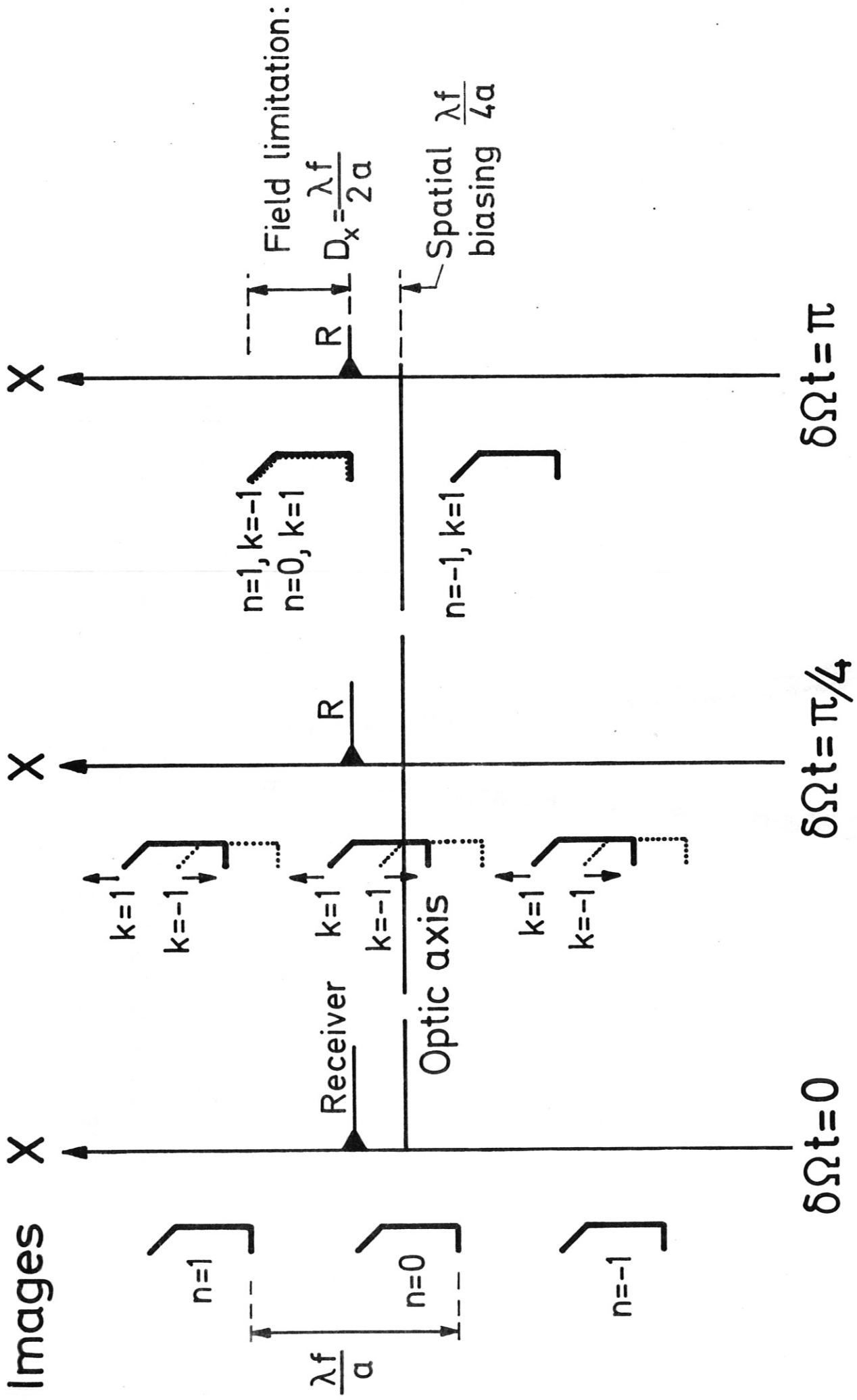
Spatial biasing $\frac{\lambda f}{4a}$

Field distribution measurements

—— by different diodes of the array

• • • by an open waveguide (arbitrary unit)
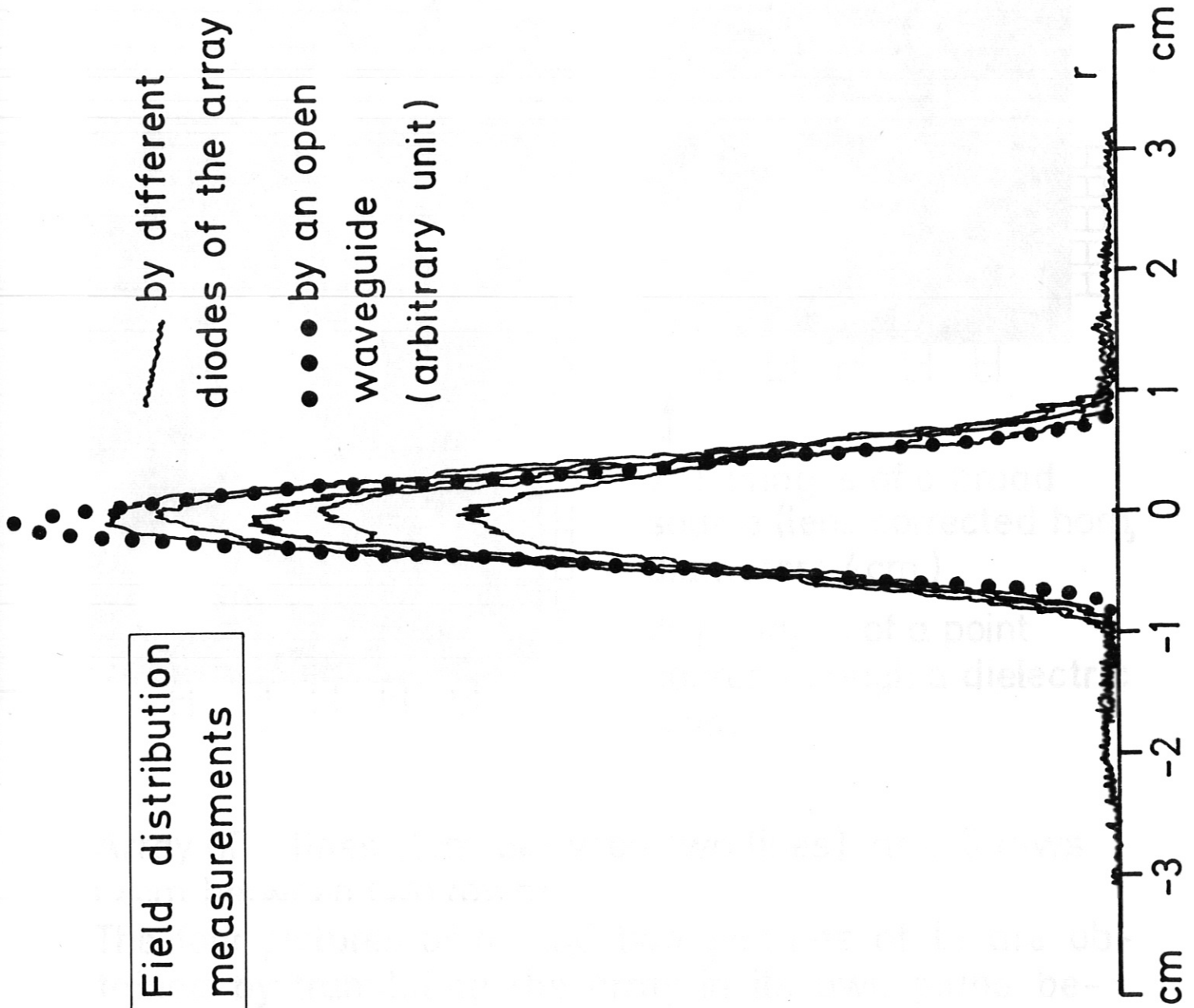
Fig. 6

Point to Point Exploration.

7b) Images of a broad source (lens corrected horn, diameter : 4cm).

← 7a) Images of a point source through a **dielectric** lens.
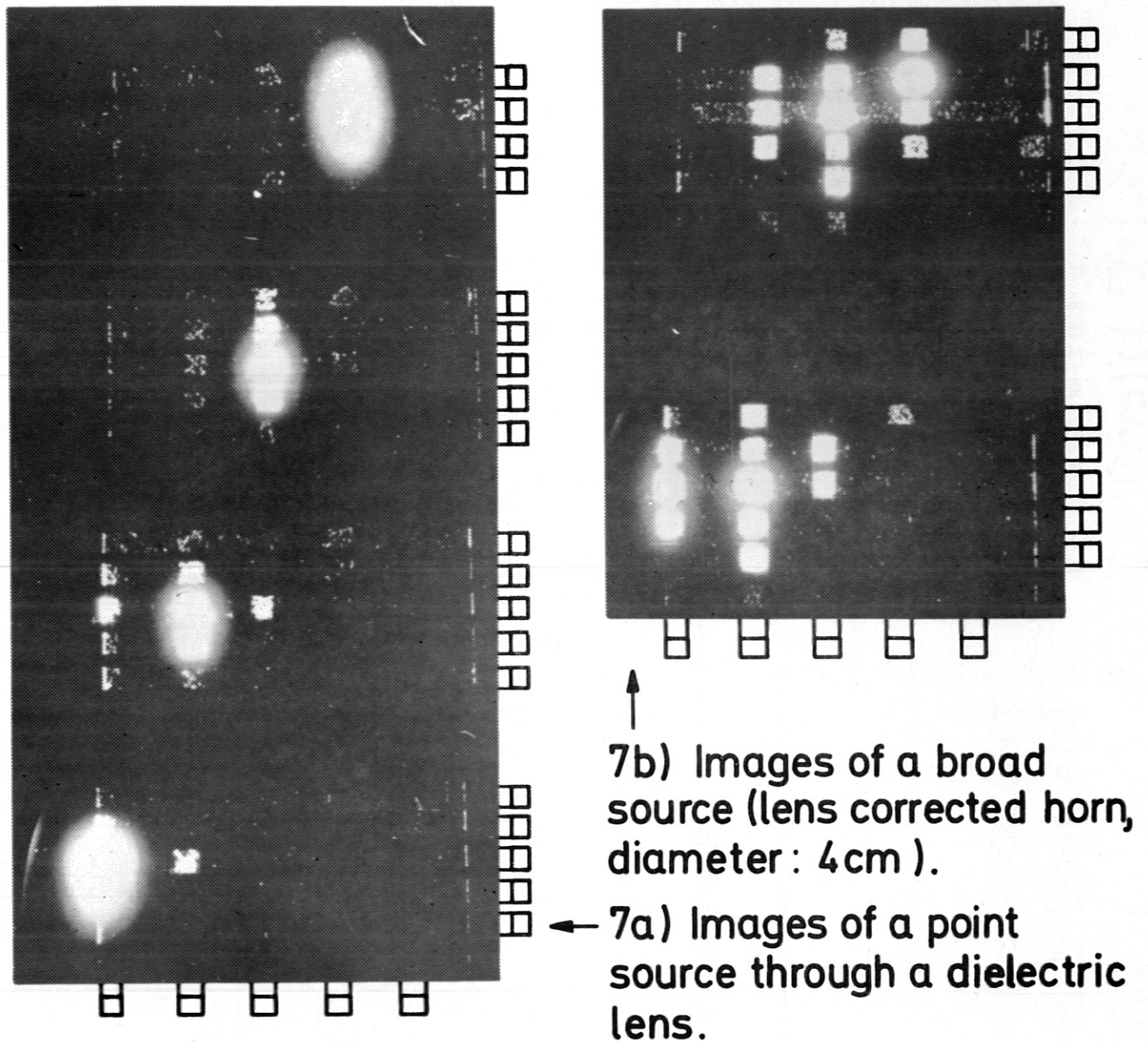
Array of 6 lines (1cm between two lines) and 5 rows (2cm between two rows).
The four pictures of a) and two pictures of b) are obtained by translating the array in its own plane between two pictures.
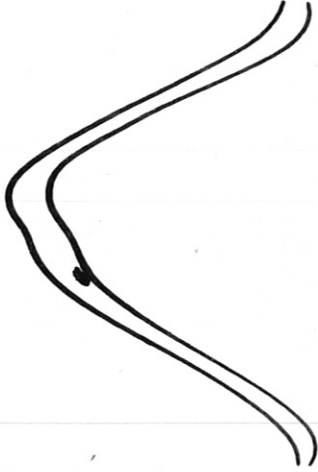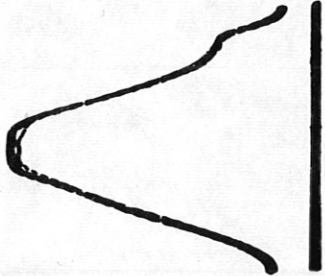
Fig. 7
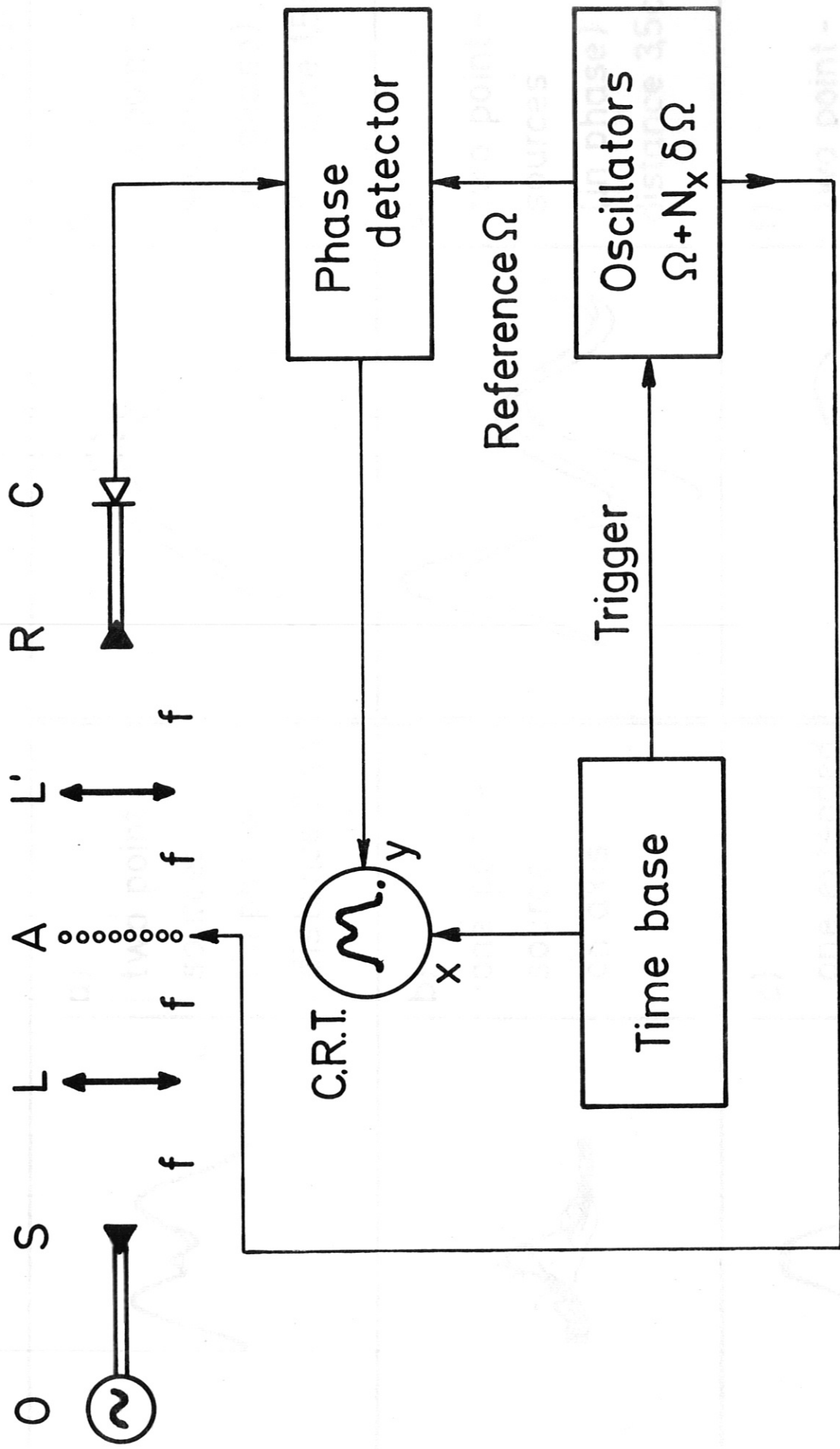
Fig. 8

O Microwave Oscillator
S Microwave Source(s)
L, L' Lenses

A Diode-array
R Receiver
C Crystal Detector

Fig. 9

a) two point-
sources
(in phase)
distance 3cm

b) one point-
source
on axis

c) one extended
source
on axis
Diam : 4cm

d) two point-
sources
(in phase)
distance 1,5cm

e) two point-
sources
(in phase)
distance 3,5cm

f) two point-
sources
(180° out of
phase)
distance 3,5cm